Supporting Information to

Fabrication of Luminescent Monolayered Tungsten Dichalcogenides Quantum Dots with Giant Spin-Valley Coupling

Liangxu Lin,[†] *Yaoxian Xu,*[‡] *Shaowei Zhan,*[§,*], *Ian M. Ross,*[] *Albert C. M. Ong,*[‡] *and Dan A. Allwood*[†,*]

†Department of Materials Science and Engineering, University of Sheffield, Sheffield S1 3JD, United Kingdom, ‡Department of Infection and Immunity, University of Sheffield, Sheffield S10 2RX, United Kingdom, §College of Engineering, Mathematics and Physical Sciences, University of Exeter, Exeter EX4 5QF, United Kingdom, and Department of Electronic and Electrical Engineering, University of Sheffield, S1 3JD, United Kingdom.

*Address correspondence to d.allwood@sheffield.ac.uk (Dan A. Allwood); s.zhang@exeter.ac.uk (Shaowei Zhang)

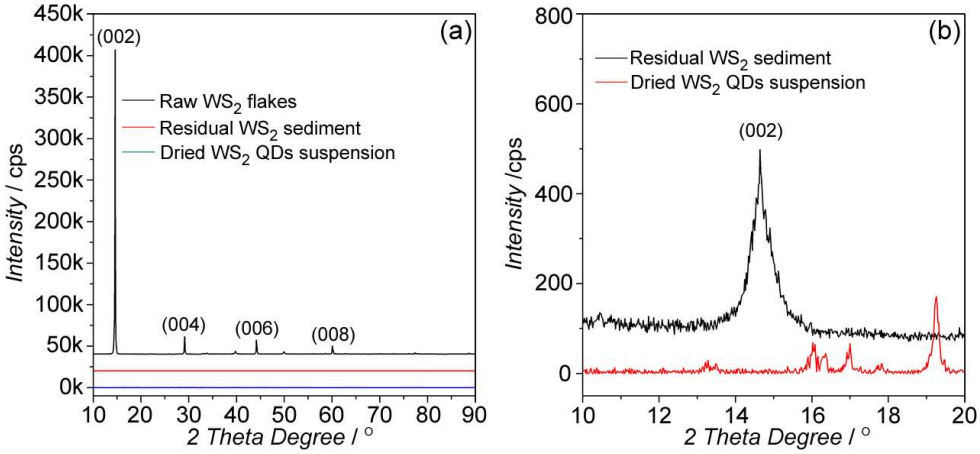

Figure S1. (a) XRD patterns of WS_2 falkes raw material, residual WS_2 sediment after preparation and dried suspension which contains WS_2 QDs. (b) Local enlarged XRD patterns of residual WS_2 sediment and dried suspension which contains WS_2 QDs. For better presentation, the zero intensities of the patterns were shifted. The diffraction peaks were indexed base on JCPDS: 84-1389. Disappearence of the (002) diffraction peak in dried suspension which contains WS_2 QDs suggest thin structure of the QDs. Due to destroy of layered structure (exfoliation and disintegration), the (002) diffraction of residual WS_2 sediment are much weakened from that of WS_2 raw materials. In the XRD pattern of dried suspension, the other diffraction peaks should from the diffractions of K salt.

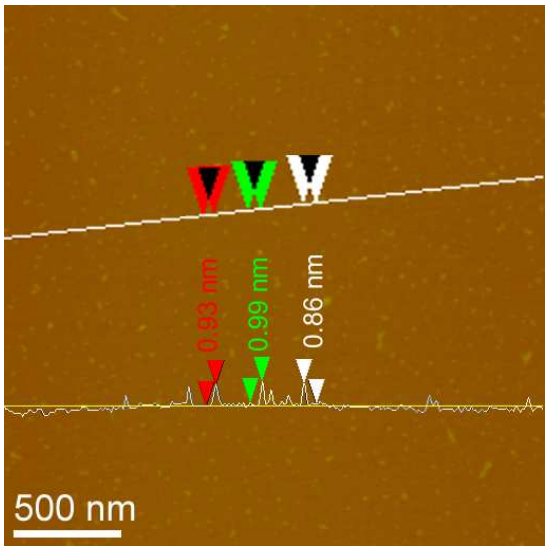

Figure S2. AFM image of WS_2 QDs. The line was plotted to across the dots' centers (three marked) to minimize measurement errors. This thickness was also proved by three-dimensional AFM image (Figure S3).

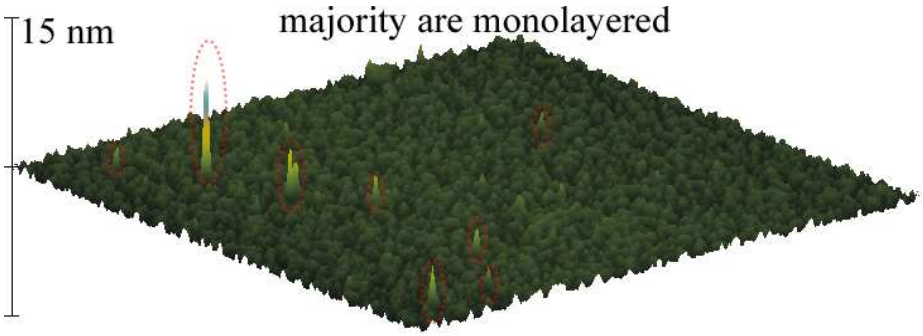

Figure S3. Three-dimensional view of the AFM image in Figure S2. The majority dots under AFM observation have same thickness (monolayered).

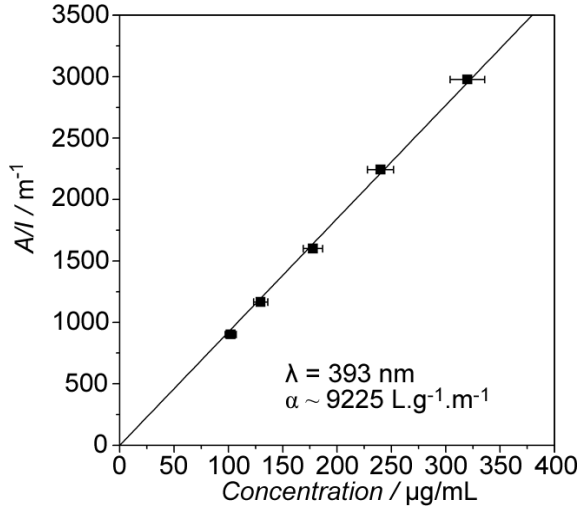

Figure S4. Plots of absorbance (λ_{ex} = 393 nm) normalized to cell length, versus the concentration of dialyzed WS_2 QDs product in water solution. The errors arise from uncertainty in the weighing and diluting processes.

Calculation of the Quantum Yield of WS_2 QDs: anthracene in ethonal (QY=0.3) was chosen as standard. The quantum yield of BN QDs (in water) was calculated according to:

$$\Phi_x = \Phi_{st}(I_x / I_{st})(\eta_x^2 / \eta_{st}^2)(A_{st} / A_x)$$

Where *Φ, I, η and A* is the quantum yield, measured integrated emission intensity, refractive index of the solvent and the optical density of the standard (*st*) anthracene and WS_2 QDs (*x*).

Table S1. Quantum yield of WS_2 QDs suspension (in H_2O) using anthracene as a reference.

Sample	Integrated Emission Intensity (*I*)	Absorptance at 360 nm (*A*)	Refractive Index of Solvent (*η*)	Quantum Yield (*Φ*)
Anthracene	286101	0.0875	1.36	30% (Known)[1-3]
WS_2 QDs	75033	0.1642	1.33	~4.0%

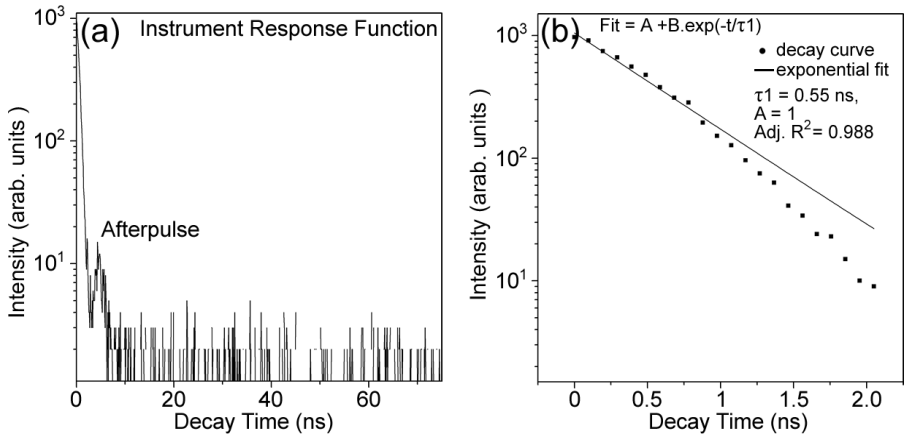

Figure S5. (a) The instrument response function. (b) The single exponential function of the instrument response (before afterpulse) showing a 0.55 ns decay time, which is different from the decay time in Figure 4b and confirmed that all the decay time in Figure 4b is not the instrument response.

Reference

1. Demas, J. N.; Grosby, G. A. The Measurement of Photoluminescence Quantum Yield. A Review. *J. Phys. Chem.* **1971**, *75*, 991-1024.

2. Dawson, W. R.; Windsor, M. W. Fluorescence Yield of Aromatic Compounds. *J. Phys. Chem.* **1968**, *72*, 3251-3260.

3. Weber, G.; Teale, F. W. J. Determination of The Absolute Quantum Yield of Fluorescent Solutions. *Trans. Faraday. Soc.* **1957**, *53*, 646-655.